A frustrated non-contact rack-pinion-rack device

2009 J. Phys.: Conf. Ser. 161 012038

(http://iopscience.iop.org/1742-6596/161/1/012038)

Journal of Physics: Conference Series **161** (2009) 012038 doi:10.1088/1742-6596/161/1/012038

A frustrated non-contact rack-pinion-rack device

MirFaez Miri

Institute for Advanced Studies in Basic Sciences, Zanjan, 45195-1159, Iran

E-mail: miri@iasbs.ac.ir

Ramin Golestanian

Department of Physics and Astronomy, University of Sheffield, Sheffield S3 7RH, UK

E-mail: r.golestanian@sheffield.ac.uk

Abstract. A design is proposed for a mechanical device made of a nanoscale pinion sandwiched without contact between two racks that exert opposing forces rooted in the quantum fluctuations of the electromagnetic field via the lateral Casimir force. The built-in frustration in the design of the system helps it to react dramatically to minute changes in the geometrical features, which suggests that it could act as a good sensor. The noncontact nature of this device could help solve the infamous wear problem in nanoscale mechanical devices.

1. Introduction

The advances in the technology of making small mechanical devices is rapidly taking us to the point where we need to worry about the tiny components in the machines wearing out too quickly [1] or sticking to each other and jamming the machines [2, 3, 4]. While a number of different strategies are being pursued to tackle these tribological issues [5], one appealing possibility is to try and take advantage of physical mechanisms of force transduction that do not involve direct contact between the components of the system.

Recently, proposals have been put forward to use the Casimir force [6, 7] for such non-contact mechanical interactions. These include both the standard normal Casimir force [8, 9] and the lateral Casimir force that appears in systems with geometrical features such as surface corrugations [10, 11]. Since the normal Casimir force is susceptible to instabilities that might be difficult to avoid in machines with small parts [2], one might argue that the lateral Casimir force between corrugated surfaces offers a more promising prospect for such applications.

Motivated by this promise, a number of designs have been recently introduced for model mechanical systems that would work at the nano-scale using the lateral Casimir force as the main force transduction mechanism. These systems include a rack-and-pinion device with the rack moving at constant speed in one direction [12], a pinion in front of a laterally vibrating rack [13], a ratchet system with a modulating gap separation [14], and a more complicated system with two racks and one pinion [15]. These designs exhibit a plethora of novel and often nonintuitive behaviors, which could help inspire the development of alternative routes to mechanical engineering at the nano-scale. Alongside with the general development of ideas for mechanical devices using the lateral Casimir force, there has also been recent significant improvements in the field theoretical calculation of the magnitude of these forces [16, 17, 18].

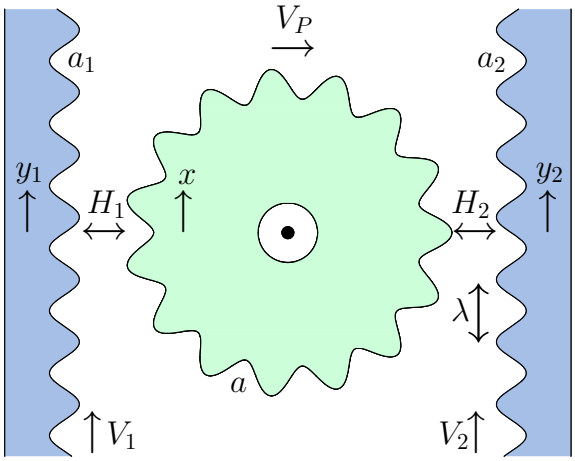

Figure 1. The schematics of the rack-pinion-rack device. The first (second) rack and the pinion have sinusoidal corrugations of wavelength λ and amplitude a_1 (a_2), and a, respectively. The choice of parallel rack velocities V_1 and V_2 (rather than opposite) frustrates the system, which is only possible because of the noncontact design. The pinion velocity V_P is taken as positive if it is in the direction shown, as a convention.

The calculation of the Casimir force is generally going to be a challenge for non-ideal geometries that might occur in the components of the small devices of the future, and we are still in need of developing theoretical formulations that can tackle this issue effectively [19].

Here, we report an extensive analysis of the behavior of a frustrated device made with two racks that are moving in the same direction, and a pinion that is coupled to them via the lateral Casimir force, as shown schematically in Fig. 1 [15]. The device has a number of geometrical features that can be controlled as parameters. Since the parameter space of the general asymmetric case is very large, we first focus on the fully symmetric device and analyze it in the dissipative regime, which is practically more relevant than the inertial regime both because it can be realized more easily and also because it will not exhibit chaotic behavior. We then focus on the heavily damped regime of the general asymmetric device, and find that the system could have five distinct behaviors: (i) the pinion could be locked with either rack-1 or rack-2, (ii) the pinion could move along with either rack-1 or rack-2 but with a lower average velocity, and (iii) the pinion could oscillate back and forth without choosing to go with either of the racks. The oscillatory regime could be used to generate a clock signal of tunable frequency.

The rest of the paper is organized as follows. Section 2 describes the general dynamical formulation of the motion of the pinion, and Sec. 3 analyzes the motion in the fully symmetric case where the problem is analytically tractable. This is followed by a report on numerical analysis of the system in it general geometrical form in Sec. 4, and some discussions in Sec. 5.

2. The Equation of Motion

The system (see Fig. 1) consists of two corrugated plates (racks) with corrugation amplitudes a_1 and a_2, separated by gaps of H_1 and H_2 from a corrugated cylinder (pinion) with corrugation amplitude a. The pinion experiences a lateral Casimir force of the form $F_{\rm lateral} = F \sin\left[2\pi(x-y)/\lambda\right]$ from each of the racks [10], where x and y represent the lateral positioning of the surfaces and λ is the wavelength of the corrugations. Note that the wavelength of the corrugations must be the same on all the three surfaces so that coherent coupling is possible. The amplitude of the lateral Casimir force F, which we can call the *Casimir grip*, depends on the geometric characteristics of the device and in particular the gap size and the amplitudes of corrugations [11, 12, 13, 20, 21, 22]. The Casimir forces from the two surface contacts add up to exert a net torque of $-RF_1 \sin\left[2\pi(x-y_1)/\lambda\right] - RF_2 \sin\left[2\pi(x+y_2)/\lambda\right]$ on the pinion, which plays a key role in the equation of motion for the principal coordinate of $x = R\theta$ that probes the dynamics of the pinion. Here θ is the angle of rotation and R is the radius of the pinion.

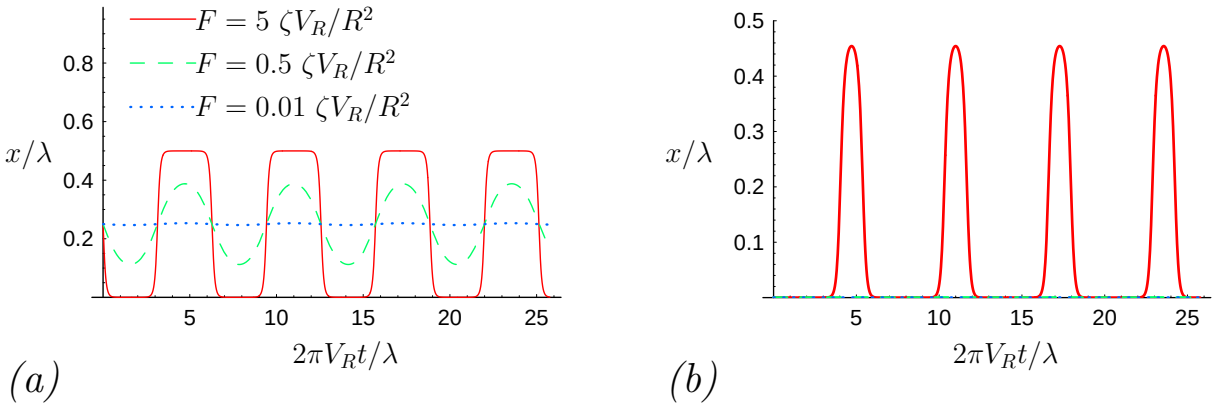

Figure 2. *(a)* Displacement of the pinion cogs as a function of time [from Eq. (4)] for the fully symmetric device, and $x_0 = 0.25\lambda$. For high values of the grip, the motion resembles a square-wave pattern. *(b)* The same (three) plots for $x_0 = 0.0001\lambda$.

Putting $y_1 = V_1 t$ and $y_2 = V_2 t$, the equation of motion reads

$$\frac{I}{R}\frac{d^2x}{dt^2} + \frac{\zeta}{R}\frac{dx}{dt} = -RF_1 \sin\left[\frac{2\pi(x - V_1 t)}{\lambda}\right] - RF_2 \sin\left[\frac{2\pi(x + V_2 t)}{\lambda}\right], \tag{1}$$

where I is the moment of inertia of the pinion about its major axis, and ζ is the rotational friction coefficient. Note that a constant offset in the argument of the sine functions in Eq. (1) due to the positioning of the pinion can be eliminated by a suitable choice of the origin for x and t. The moment of inertia of the pinion can be estimated as $I = \frac{1}{2}MR^2 = \frac{\pi}{2}\rho L R^4$, assuming it is a cylinder of mass M and density ρ, with L being the thickness (or height) of the pinion. We can also estimate the rotational friction coefficient ζ assuming that the main source of friction in the system comes from the lubrication at the axle (or pivot) on which the pinion is mounted. For an axle of radius r that is lubricated with a fluid layer of thickness h and viscosity η, we find $\zeta \simeq 2\pi\eta L r^3/h$.

We can gauge the relative importance of the inertial term and the friction term on the left hand side of Eq. (1), by scaling out the relevant dimensional parameters. We find that the ratio between the inertial term and the friction term is controlled by the dimensionless parameter $I^* \equiv 2\pi IV/(\zeta\lambda)$ where V is a typical rack velocity. We thus find that for $V \ll V_\times$, with the *crossover velocity* being defined as

$$V_\times = \frac{\zeta\lambda}{2\pi I} = \frac{2\eta\lambda r^3}{\pi\rho h R^4}, \tag{2}$$

the dynamics of the system is primarily controlled by the friction term, and the inertial term can be safely ignored. Using $\rho = 1.17$ gr/cm^3 (for silicone), $\eta = 10^{-3}$ Pa.s (for a lubricant as thick as water), and the geometrical parameters as $R = 1$ μm, $\lambda = 500$ nm, $r = 500$ nm, and $h = 100$ nm, we find $V_\times = 0.34$ m/s. In this paper we are going to assume that this condition is fulfilled, and study the dynamics of the system in the heavily damped limit.

The system has four tunable parameters: two rack velocities of V_1 and V_2 that can be directly controlled, and two Casimir grips of F_1 and F_2 that can be tuned by the gap sizes H_1 and H_2. We first consider the fully symmetric case where $V_1 = V_2$ and $F_1 = F_2$ due to its simplicity.

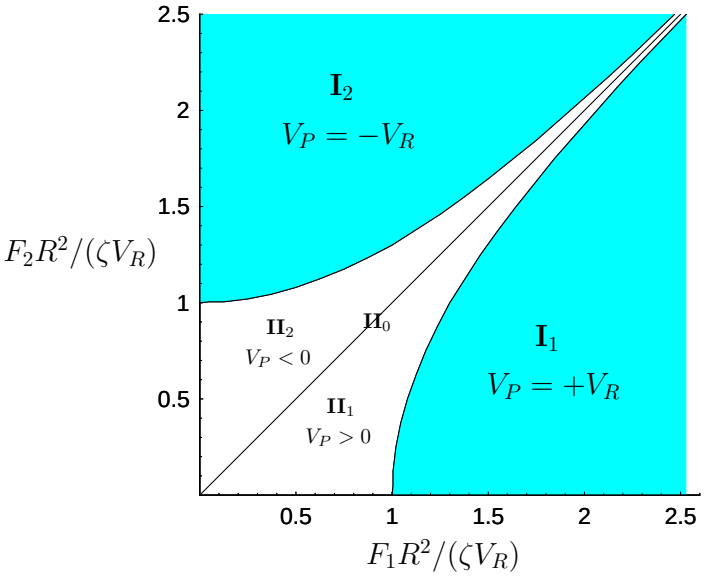

Figure 3. Phase diagram for the motion of the pinion, corresponding to $V_R = V_1 = V_2$. There are five different behaviors: $V_P = +V_R$ locked to the first rack, $V_P > 0$ moving with the first rack with skipping, $V_P = -V_R$ locked to the second rack, and $V_P < 0$ moving with the second rack with skipping. On the line $F_1 = F_2$ the pinion has a neutral oscillatory motion.

3. The Fully Symmetric Case

In the fully symmetric case of $V_R \equiv V_1 = V_2$ and $F \equiv F_1 = F_2$, the equation of motion reads

$$\frac{dx}{dt} = -2\left(\frac{R^2F}{\zeta}\right)\sin\left(\frac{2\pi x}{\lambda}\right)\cos\left(\frac{2\pi V_R t}{\lambda}\right), \tag{3}$$

and is symmetric under the transformation $x \leftrightarrow -x$. It follows that the pinion cannot choose a sense of rotation over the other, and thus performs purely oscillatory motion. Due to its simplicity, in this case the equation of motion can be solved analytically to yield

$$x = \frac{\lambda}{\pi}\tan^{-1}\left\{\tan\left(\frac{\pi x_0}{\lambda}\right)\exp\left[-\frac{2R^2F}{\zeta V_R}\sin\left(\frac{2\pi V_R t}{\lambda}\right)\right]\right\}, \tag{4}$$

where x_0 is the initial position of the pinion. Note that the sign of x_0 determines the sign of the whole solution $x(t)$. Equation (4) is plotted in Fig. 2 for different values of the Casimir grip F and the initial pinion position. It shows that the device can generate interesting periodic patterns such as a nearly perfect square wave or a train of spikes, with a frequency V_R/λ that can be easily controlled by the rack velocity. The solution [Eq. (4)] involves an exponential amplification factor that is controlled by the Casimir grip, which could help detect incredibly small displacements. This can be seen in the example plotted in the inset of Fig. 2, which shows a 10^4-fold amplification for $F = 5\ \zeta V_R/R^2$.

4. The General Case

The equation of motion for a general heavily damped rack-pinion-rack device reads

$$\frac{\zeta}{R^2}\frac{dx}{dt} = -F_1\sin\left[\frac{2\pi(x - V_1 t)}{\lambda}\right] - F_2\sin\left[\frac{2\pi(x + V_2 t)}{\lambda}\right]. \tag{5}$$

Equation (5) is symmetric under the combined transformation of $V_1 \leftrightarrow V_2$, $F_1 \leftrightarrow F_2$, and $x \leftrightarrow -x$. This symmetry greatly simplifies our numerical study of the behavior of the device in its large parameter space.

First we consider the case of equal rack velocities $V_R \equiv V_1 = V_2$. We expect our system to inherit the behavior of the previously studied design of a rack and pinion using the lateral

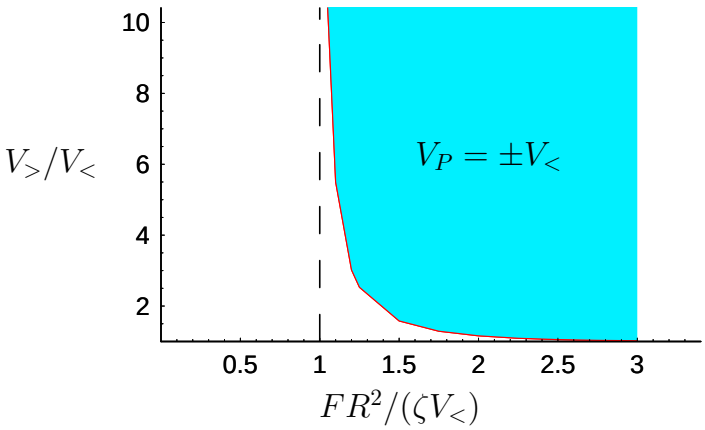

Figure 4. Phase diagram for the motion of the pinion, corresponding to $F \equiv F_1 = F_2$. In the region $V_P = \pm V_<$ the pinion is locked to the rack whose velocity is lower. Note that the phase boundary is about to asymptote to the horizontal line $V_>/V_< = 1$ at high values of $FR^2/(\zeta V_<)$.

Casimir force [12, 22]: The pinion can be locked onto a rack moving at a given velocity, if the friction force for such velocities can be balanced by the available Casimir grip. This means that the Casimir grips F_1 and F_2 introduce two *skipping* velocities $V_{S1} \sim F_1 R^2/\zeta$ and $V_{S2} \sim F_2 R^2/\zeta$. In the case of $F_2 < F_1$ and $V_R < V_{S1}$ ($F_1 < F_2$ and $V_R < V_{S2}$) it is possible for the pinion to lock onto the first (second) rack. Numerical studies summarized in Fig. 3 confirm our expectation. Figure 3 delineates the domains where the pinion is locked, as well as the phase boundary for the skipping transition. The system exhibits five different behaviors ranging from the pinion being locked to rack-1 (I_1) or rack-2 (I_2) to motion with skipping along rack-1 (II_1) or rack-2 (II_2). The phase boundary between the two II-phases (denoted in Fig. 3 as II_0) corresponds to the vanishing of the net pinion velocity and thus an oscillatory behavior similar to the symmetric device as described by the solution in Eq. (4) and Fig. 2. As expected, this phase diagram is symmetric with respect to the line $F_1 = F_2$.

In the case of equal forces $F \equiv F_1 = F_2$, the pinion follows one of the racks — the one whose velocity is lower — provided that the friction force for such velocities can be balanced by the available Casimir grip. It is natural to introduce $V_> = \mathrm{maximum}(V_1, V_2)$ and $V_< = \mathrm{minimum}(V_1, V_2)$ and present the phase diagram of the system in terms of $V_>/V_<$ and $FR^2/(\zeta V_<)$, although the symmetry of Eq. (5) under the combined transformation of $V_1 \leftrightarrow V_2$ and $x \leftrightarrow -x$ is not manifest. Figure 4 demonstrates the domains where the pinion is locked, as well as the phase boundary for the skipping transition. Note that the phase boundary of Fig. 4 is about to asymptote to a vertical line at small values of F or large values of $V_<$ (i.e. when the skipping velocity is quite small). The phase boundary also asymptotes to the horizontal line $V_>/V_< = 1$ at high values of $FR^2/(\zeta V_<)$. This implies that at large values of the Casimir grip F or small gap size H, the pinion motion is extremely sensitive and can reveal a slight difference in the rack velocities.

We have also studied the behavior of the device in the case of unequal Casimir grips and unequal rack velocities. Figure 5 shows a representative phase diagram for a specific section of the space of parameters. It can be seen that the system again exhibits the same five different behaviors: locked to rack-1 (I_1) or rack-2 (I_2), motion with skipping along rack-1 (II_1) or rack-2 (II_2), or oscillatory motion. The phase boundary between the two II-phases (shown in Fig. 5 as a dashed line and denoted as II_0) corresponds to the vanishing of the net pinion velocity and thus an oscillatory behavior similar to the symmetric device as described by the solution in Eq. (4) and Fig. 2. Note that the phase boundary between I_1 and II_1 in Fig. 5 is about to asymptote to a vertical line at lower values of F_1 below which the phase I_1 cannot exist (corresponding to V_{S1} discussed above). The inset of Fig. 5 shows the average pinion velocity for a typical section of the phase diagram (shown as dash-dotted line in Fig. 5), going from $V_P = -V_2$ to $V_P = V_1$ passing through two sharp transition points and zero. The singular nature of the

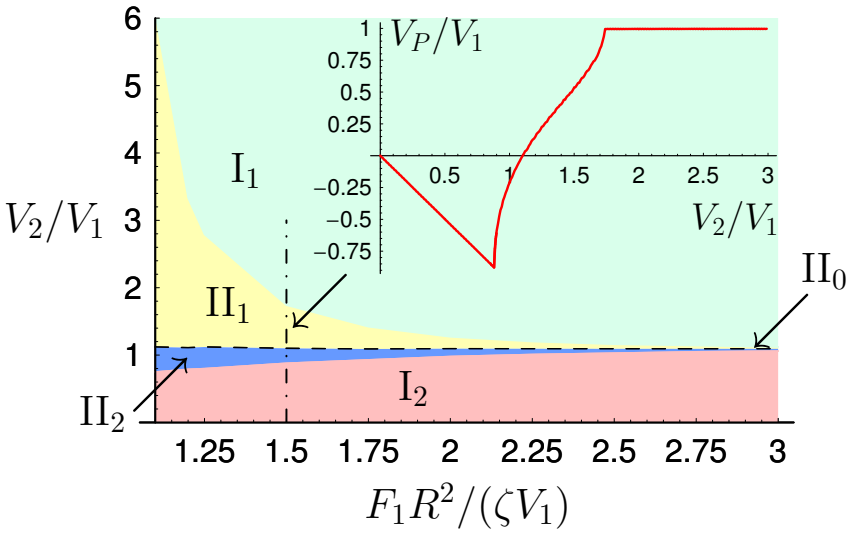

Figure 5. Phase diagram for the motion of the pinion, corresponding to $F_2 = F_1 + 0.05\ \zeta V_1/R^2$. There are five different behaviors: I_1 locked with rack-1, II_1 moving with rack-1 with skipping, II_0 neutral oscillatory motion (dashed line), II_2 moving with rack-2 with skipping, and I_2 locked with rack-2. Inset: pinion velocity versus rack velocity for $F_1 = 1.50\ \zeta V_1/R^2$ and $F_2 = 1.55\ \zeta V_1/R^2$ (corresponding to a vertical cut of the phase diagram at the dash-dotted line) showing the five different regimes.

skipping transitions is manifest in the cusps that appear in the velocity profile at the location of the two transitions.

5. Discussion

The rack-pinion-rack device demonstrates a rich variety of possible behaviors that are all possible thanks to the noncontact nature of the design and the built-in frustration. A key parameter in the system seems to be the skipping transition velocity which determines the limit of velocity that can be tolerated by the system in the locked phase.

We can estimate the skipping velocities using typical values for the Casimir grip, which in its turn is determined by the gap size and other geometrical and material features of the device [11, 12, 13, 20, 21]. For typical (and experimentally realized [23]) values of $a = 50$ nm (assumed for all surfaces) and $\lambda = 500$ nm, we find $F = 0.3$ pN for $H = 200$ nm assuming the boundaries are perfect metals. This yields a skipping velocity of $V_S \sim FR^2/\zeta = 3.8\ \mu$m/s. However, reducing the gap size (by only a factor of **two**) to $H = 100$ nm yields $F = 12$ pN and consequently $V_S \sim FR^2/\zeta = 150\ \mu$m/s (that is enhanced by a factor of **forty**). In practical situations with real metallic boundaries of smaller reflectivity, the Casimir grip tends to be slightly weaker, but the general behavior of the system will still be the same.

The clock signal is a particularly appealing feature of the device, which is the result of perfect balance between the forces in the system. Interestingly, such a signal does not necessarily need to come from the fully symmetric device, and as the phase diagram of Fig. 5 shows it can be obtained by tuning the system into the dashed line (II_0) transition boundary for any geometrical design. To get a strong coupling signal like the square wave or the train of spikes shown in Fig. 2, we need to have a rack velocity of say $V_R = FR^2/(5\zeta)$, which is equal to 30 μm/s for $H = 100$ nm. This yields $f = V_R/\lambda = 60$ Hz using the above value for the corrugation wavelength. Higher rack velocities can lead to higher frequencies, although the shape of the signal will change to a simple sinusoidal one as the coupling gets weaker progressively with increasing rack velocity.

In conclusion,, we have employed the coupling between corrugated surfaces due to the lateral Casimir force to propose a nanoscale mechanical device composed of two racks and a pinion. The noncontact nature of the interaction allows for the system to be made frustrated, which leads to a rich and sensitive phase behavior. Most notably, we have found that the device could be potentially useful as a mechanical sensor or amplifier, and it could also be used to make a mechanical clock signal of tunable frequency. The noncontact nature of this device, and other variants based on similar principles, could help in solving the wear problem in nano-scale mechanical devices.

Acknowledgments

One of us (RG) would like to thank Victor Dodonov and other organizers of the international workshop *60 Years of Casimir Effect* in Brasilia, for creating such a memorable event. It is a pleasure to acknowledge fruitful discussions with R.A.L. Jones. This work was supported by EPSRC under Grant EP/F036167/1.

References

[1] de Boer M P and Mayer T M 2001 *MRS Bull.* **26** 302
[2] Buks E and Roukes M L 2001 *Phys. Rev.* B **63** 033402
[3] Socoliuc A, Gnecco E, Maier S, Pfeiffer O, Baratoff A, Bennewitz R and Meyer E 2006 *Science* **313** 207
[4] Park J Y, Ogletree D F, Thiel P A and Salmeron M 2006 *Science* **313** 186
[5] Carpick R W 2006 *Science* **313** 184
[6] Casimir H B G 1948 *Proc. K. Ned. Akad. Wet.* **51** 793
[7] Bordag M, Mohideen U and Mostepanenko V M 2001 *Phys. Rep.* **353** 1
[8] Chan H B, Aksyuk V A, Kleiman R N, Bishop D J and Capasso F 2001 *Science* **291** 1941
[9] Chan H B, Aksyuk V A, Kleiman R N, Bishop D J and Capasso F 2001 *Phys. Rev. Lett.* **87** 211801
[10] Golestanian R and Kardar M 1997 *Phys. Rev. Lett.* **78** 3421
[11] Chen F, Mohideen U, Klimchitskaya G L and Mostepanenko V M 2002 *Phys. Rev. Lett.* **88** 101801
[12] Ashourvan A, Miri M F and Golestanian R 2007 *Phys. Rev. Lett.* **98** 140801
[13] Ashourvan A, Miri M F and Golestanian R 2007 *Phys. Rev.* E **75** 040103 (R)
[14] Emig T 2007 *Phys. Rev. Lett.* **98** 160801
[15] Miri M F and Golestanian R 2008 *Appl. Phys. Lett.* **92** 113103
[16] Lombardo F C, Mazzitelli F D and Villar P I 2008 *J. Phys. A* **41** 164009
[17] Cavero-Peláez I, Milton K A, Parashar P and Shajesh K V 2008 *Phys. Rev.* D **78** 065018
[18] Cavero-Peláez I, Milton K A, Parashar P and Shajesh K V 2008 *Phys. Rev.* D **78** 065019
[19] For an example, see: Golestanian R 2005 *Phys. Rev. Lett.* **95** 230601
[20] Emig T, Hanke A, Golestanian R and Kardar M 2003 *Phys. Rev. A* **67** 022114
[21] Rodrigues R B, Maia Neto P A, Lambrecht A and Reynaud S 2006 *Phys. Rev. Lett.* **96** 100402
[22] Ashourvan A, Miri M F and Golestanian R 2007 *J. Phys.: Conf. Ser.* **89** 012017
[23] Mohideen U 2008 *private communication*